Near-field localization of ultrashort optical pulses in transverse 1-D periodic nanostructures

Wataru Nakagawa, Rong-Chung Tyan, Pang-Chen Sun, and Yeshaiahu Fainman

Department of Electrical and Computer Engineering, University of California, San Diego
9500 Gilman Drive, La Jolla, CA 92093-0407
wnakagaw@ucsd.edu, fainman@ece.ucsd.edu

Abstract: We present a transverse 1-D periodic nanostructure which exhibits lateral internal field localization for normally incident ultrashort pulses, and which may be applied to the enhancement of nonlinear optical phenomena. The peak intensity of an optical pulse propagating in the nanostructure is approximately 12 times that of an identical incident pulse propagating in a bulk material of the same refractive index. For second harmonic generation, an overall enhancement factor of approximately 10.8 is predicted. Modeling of pulse propagation is performed using Fourier spectrum decomposition and Rigorous Coupled-Wave Analysis (RCWA).

© 2000 Optical Society of America

OCIS codes: (050.1970) diffractive optics; (190.4420) nonlinear optics, transverse effects in; (230.3990) microstructure devices; (999.9999) ultrashort pulses; (999.9999) optical nonlinearity enhancement

References and links

1. P. Lalanne and J.-P. Hugonin, "High-order effective-medium theory of subwavelength gratings in classical mounting: application to volume holograms," J. Opt. Soc. Am. A **15,** 1843–1851 (1998).
2. J. N. Mait, D. W. Prather, and M. S. Mirotznik, "Design of binary subwavelength diffractive lenses by use of zeroth-order effective-medium theory," J. Opt. Soc. Am. A **16,** 1157–1167 (1999).
3. F. Xu, R.-C. Tyan, P.-C. Sun, Y. Fainman, C.-C. Cheng, and A. Scherer, "Form-birefringent computer-generated holograms," Opt. Lett. **21,** 1513–1515 (1996).
4. R.-C. Tyan, A. A. Salvekar, H.-P. Chou, C.-C. Cheng, A. Scherer, P.-C. Sun, F. Xu, and Y. Fainman, "Design, fabrication and characterization of form-birefringent multilayer polarizing beam splitter," J. Opt. Soc. Am. A **14,** 1627–1636 (1997).
5. J. E. Sipe and R. W. Boyd, "Nonlinear susceptibility of composite optical materials in the Maxwell Garnett model," Phys. Rev. A **46,** 1614–1629 (1992).
6. R. W. Boyd and J. E. Sipe, "Nonlinear optical susceptibilities of layered composite materials," J. Opt. Soc. Am. B **11,** 297–303 (1994).
7. G. L. Fischer, R. W. Boyd, R. J. Gehr, S. A. Jenekhe, J. A. Osaheni, J. E. Sipe, and L. A Weller-Brophy, "Enhanced nonlinear optical response of composite materials," Phys. Rev. Lett. **74,** 1871–1874 (1995).
8. R. S. Bennink, Y.-K. Yoon, R. W. Boyd, and J. E. Sipe, "Accessing the optical nonlinearity of metals with metal-dielectric photonic bandgap structures," Opt. Lett. **24,** 1416–1418 (1999).
9. K. P. Yuen, M. F. Law, K. W. Yu, and P. Sheng, "Enhancement of optical nonlinearity through anisotropic microstructures," Opt. Comm. **148,** 197–207 (1998).
10. H. Ma, R. Xiao, and P. Sheng, "Third-order optical nonlinearity enhancement through composite microstructures," J. Opt. Soc. Am. B 15, 1022–1029 (1998).
11. M. G. Moharam and T. K. Gaylord, "Diffraction analysis of dielectric surface-relief gratings," J. Opt. Soc. Am. **72,** 1385–1392 (1982)
12. N. Chateau and J.-P. Hugonin, "Algorithm for the rigorous coupled-wave analysis of grating diffraction," J. Opt. Soc. Am. A **11,** 1321–1331 (1994).
13. M. G. Moharam, D. A. Pommet, E. B. Grann, and T. K. Gaylord, "Stable implementation of the rigorous coupled-wave analysis for surface-relief gratings: enhanced transmittance matrix approach," J. Opt. Soc. Am. A **12,** 1077–1086 (1995).
14. L. Li, "Formulation and comparison of two recursive matrix algorithms for modeling layered diffraction gratings," J. Opt. Soc. Am. A **13,** 1024–1035 (1996).
15. M. Schmitz, R. Bräuer, O. Bryngdahl, "Comment on numerical stability of rigorous differential methods of diffraction," Opt. Comm. **124,** 1–8 (1996).

#22950 - $15.00 US Received June 02, 2000; Revised July 26, 2000
(C) 2000 OSA

16. R. Tyan, “Design, modeling and characterization of multifunctional diffractive optical elements,” Ph.D. Thesis, University of California, San Diego (1998).
17. W. Nakagawa, R.-C. Tyan, P.-C. Sun, F. Xu, and Y. Fainman, “Ultrashort pulse propagation in near-field periodic diffractive structures using Rigorous Coupled-Wave Analysis,” submitted to J. Opt. Soc. Am. A (2000).

1. Introduction

Near-field effects in subwavelength diffractive optical structures (optical nanostructures) have played an important role in a variety of optics and photonics technologies, including artificial materials [1,2], polarization-selective devices based on form birefringence [3,4] and nonlinearity enhancement in composite materials [5–10]. In each of these cases, the unique optical properties of the device derive from the strong influence of the nanoscale structure on the optical near fields. For a variety of applications, it is desirable to employ these near-field nanostructures in conjunction with ultrashort optical pulses—for example, in integrated optical communications systems to increase data rates or to enable all-optical switching through nonlinear optical effects. However, to the best of our knowledge, the interaction of ultrashort pulses and near-field optical nanostructures has not yet been thoroughly investigated.

In this manuscript, we apply our recently-developed tool for the analysis of ultrashort pulse propagation in periodic diffractive nanostructures to study an important near-field effect: lateral localization of ultrashort optical pulses propagating in a transverse 1-D periodic nanostructure. Ultrashort optical pulses are widely used in the study of nonlinear optical phenomena due to their extremely high peak power—since the output of a nonlinear optical process scales as the square or higher power of the input, temporal localization of the pulse energy results in an overall enhancement of the nonlinear effect. Similarly, transverse localization of the pulse energy in a nanostructure will lead to a further increase in the peak power of the pulse, and consequently further enhancement of the nonlinear effect. We present a design for a subwavelength 1-D periodic nanostructure which exhibits strong transverse field localization in the high index region for a TE-polarized incident optical pulse.

In order to investigate ultrashort laser pulse propagation in optical nanostructures, we have developed a modeling tool to analyze the interaction of ultrashort optical pulses with periodic subwavelength diffractive structures based on the integration of two proven analysis methods: Fourier spectrum decomposition and the Rigorous Coupled-Wave Analysis method (RCWA) [11]. In Section 2, we briefly describe this extension of the RCWA method to model ultrashort pulse propagation. In Section 3, we describe the transverse field localization structure, and in Section 4, we discuss its application to the enhancement of nonlinear optical phenomena. A summary of the results and conclusions are presented in Section 5.

2. Modeling method

The Rigorous Coupled-Wave Analysis [11] method is a well-established tool for characterization of monochromatic wave propagation through periodic diffractive nanostructures. However, since an ultrashort pulse contains a broad optical frequency spectrum, it is necessary to extend the existing RCWA method to analyze polychromatic fields. We consider the propagation of an infinite periodic sequence of Gaussian ultrashort pulses and use Fourier methods to obtain the corresponding spectrum, consisting of a number of discrete frequency components. These discrete components are independently analyzed using a modified RCWA technique (various modifications have been made to the original RCWA method [11] to facilitate stable numerical solution [12–15] and explicit computation of the internal fields of the nanostructure [16,17]). The resulting monochromatic diffracted fields are then coherently superimposed to produce the time-domain solution, revealing the interaction between the ultrashort pulses and the periodic diffractive nanostructure.

#22950 - $15.00 US Received June 02, 2000; Revised July 26, 2000
(C) 2000 OSA

We assume an incident infinite periodic train of Gaussian pulses as shown in Eq. (1), corresponding to the output of typical ultrashort pulse laser systems:

$$\vec{E}(\vec{r}, t) = \left\{ \hat{a}_0 \exp\left[\frac{(t - (\hat{k}_0 \cdot \vec{r})/v_g - t_0)^2}{2\tau^2} \right] \exp[-j(\vec{k}_0 \cdot \vec{r} - \omega_0 t)] \right\} \otimes \sum_{n=-\infty}^{\infty} \delta(t - n\Delta T) \quad (1)$$

where $\vec{r}$ and t are space and time coordinates, respectively, $\hat{a}_0$ indicates the polarization of the incident pulse, ω_0 is the center frequency of the pulse, $\vec{k}_0$ is the wave vector corresponding to the center frequency of the pulse, $\hat{k}_0$ is a unit vector in the direction of $\vec{k}_0$, v_g is the group velocity of the pulse, τ is the width parameter of the Gaussian pulse envelope, t_0 is the time at which the pulse peak arrives at $\vec{r} = 0$, ΔT is the temporal separation between pulses in the incident pulse train, $\otimes$ indicates the convolution operation, and n is an integer. Taking the Fourier transform of Eq. (1) and imposing a finite truncated bandwidth $\Delta\omega = 2M \cdot \delta\omega$ centered at ω_0, we obtain

$$\tilde{E}(\vec{r}, \omega) = \hat{a}_0 \sqrt{2\pi}\tau \exp\left[-j\vec{k}_0 \cdot \vec{r} - j\Omega\left(\frac{\hat{k}_0 \cdot \vec{r}}{v_g} + t_0 \right) - \frac{\tau^2 \Omega^2}{2} \right] \cdot \sum_{n=-M}^{M} \delta(\Omega - n\delta\omega), \quad (2)$$

where $\Omega = \omega - \omega_0$ and $\delta\omega = 2\pi/\Delta T$. Eq. (2) is a finite, discrete frequency-domain representation of the incident fields having $2M + 1$ discrete frequency components over index n (where $n = \{-M, \ldots, 0, \ldots, M\}$) at frequencies $\omega_n = \omega_0 + n\delta\omega$. Thus, for each component, the RCWA method can be applied to solve for the diffracted fields.

For each frequency component, the RCWA method yields the resulting reflected, transmitted, or internal fields of the grating. To obtain the time domain solution for the fields, we must coherently superpose the fields corresponding to each frequency component. This superposition corresponds to the inverse of the Fourier transform performed in obtaining Eq. (2) from Eq. (1). Since the frequency-domain representation of the fields in Eq. (2) is discrete, we apply a discrete inverse Fourier transform, yielding the field at a particular point in space and time. In practice, the superposition is carried out for an array of points, and the results introduced into a variety of visualization tools for analysis and interpretation.

In the following example, we assume a typical femtosecond laser pulse of width 167 fs FWHM, corresponding to a Gaussian width parameter of $\tau = 1 \times 10^{-13}$ sec. The temporal separation between pulses in the incident pulse train is assumed to be $\Delta T = 50$ ps, corresponding to a frequency sampling interval of $\delta\omega = 4\pi \times 10^{10}$ rad. We also choose a truncated bandwidth of $\Delta\omega = 3\pi \times 10^{13}$ rad, corresponding to $2M + 1 = 751$ discrete spectral components. Although a frequency-dependent material refractive index can easily be incorporated due to the spectral decomposition, in this manuscript the effects of material dispersion are omitted for simplicity.

3. Transverse field localization

We apply this tool to analyze pulse propagation in a subwavelength 1-D periodic nanostructure which exhibits strong transverse field localization within each period of the structure. For a

#22950 - $15.00 US Received June 02, 2000; Revised July 26, 2000
(C) 2000 OSA

center wavelength of $\lambda = 1.0$ μm, we have chosen the subwavelength 1-D grating to have a period of $\Lambda = 0.65$ μm and a fill factor of $F = 0.09$, as shown in Fig. 1. For clarity, the depth of the structure is chosen to be $d = 100$ μm to avoid the introduction of interference effects in the propagation direction. The refractive indices of the grating materials are assumed to be $n_1 = 3.5$ in the high index region (corresponding to the properties of GaAs) and $n_2 = 1.0$ in the air gap. The incident pulse train is assumed to be normally incident.

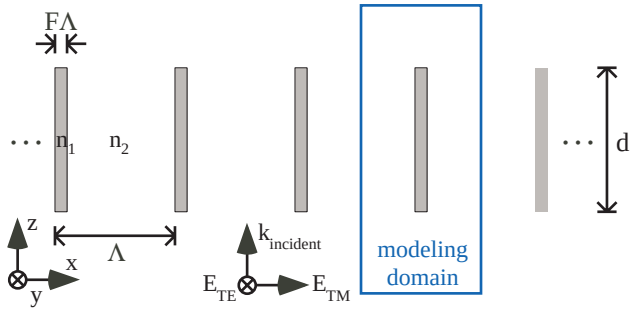

Fig. 1. Schematic diagram of the transverse field localization nanostructure: an infinitely periodic square subwavelength grating with period Λ, fill factor F, and depth d.

Figs. 2a and 2b respectively show the propagation of TE- and TM-polarized 167 fs FWHM ultrashort optical pulses through the nanostructure described above. Note that although the incident pulses have uniform transverse profiles, inside the grating structure the pulses exhibit strong transverse localization. In the TE case, the majority of the pulse energy is localized in the high refractive index region, while in the TM case the pulse energy is found in the air gap. The peak value of the squared magnitude of the electric field ($|E|^2$) inside the nanostructure occurs for the TE polarization, and is approximately 2.4 times that of the incident pulse. Despite the localization inside the structure, the transmitted and reflected pulses have uniform transverse profiles due to the subwavelength scale of the nanostructure.

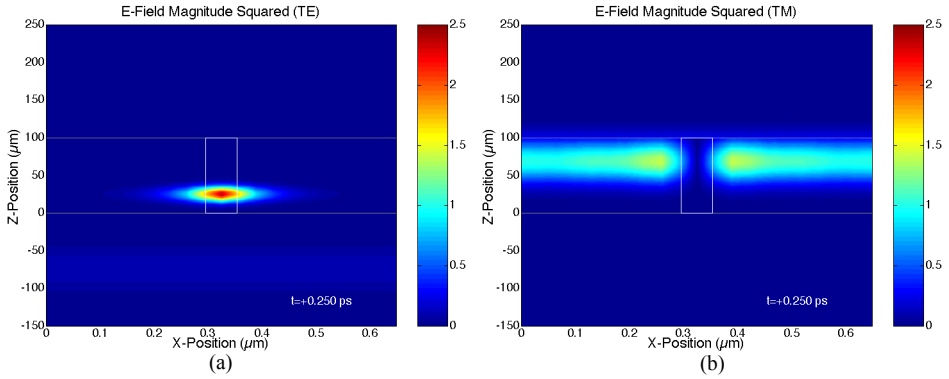

Fig. 2. Normalized squared magnitude of the electric field of an ultrashort optical pulse (center wavelength 1.0 μm, 167 fs FWHM) propagating inside the structure shown in Fig. 1. Each movie shows one period of an infinitely periodic structure for: (a) (2.5 MB) TE polarized incident pulse and (b) (2.0 MB) TM polarized incident pulse.

#22950 - $15.00 US
Received June 02, 2000; Revised July 26, 2000
(C) 2000 OSA

The TE- and TM-polarized pulses exhibit radically different transverse profiles due to the differing boundary conditions imposed on the near fields by the nanostructure. For the TM polarization (i.e. with electric field in the $\hat{x}$-direction as shown in Fig. 1), the boundary condition at the grating groove interfaces requiring continuity of the normal component of the electric displacement results in a stronger electric field in the low index region of the grating. Since the grating has a subwavelength period, this effect results in transverse localization of most of the pulse energy in the low refractive index material, with the highest field magnitude being observed nearest the interfaces. Alternatively, for the TE polarization (i.e. with electric field in the $\hat{y}$-direction as shown in Fig. 1), the boundary conditions require continuity of the tangential electric fields, imposing no particular transverse profile on the field. However, the mode structure of the coupled waveguide array results in transverse localization of the field energy in the high refractive index material, in a similar fashion to the mode profile of a single-mode slab waveguide. Since most commonly used bulk nonlinear optical materials tend to have relatively high indices of refraction, it is the TE polarization case—where the pulse energy is localized in the high refractive index region of the grating—that is of interest.

4. Enhancement of nonlinear optical phenomena

In order to apply the transverse localization effect to the enhancement of nonlinear optical phenomena, we must first find the optimum transverse field profile. Due to the near-field nature of the transverse localization effect, we expect the degree of field localization to be extremely sensitive to the dimensions of the structure. Fig. 3 shows the transverse profile of $|E|^2$ at the pulse peak for five nanostructures having the same period (Λ = 0.65 μm) but differing fill factors: 1%, 3%, 6%, 9%, and 12%, as well as the bulk case (100%). For very small fill factors (e.g. the 1% case), the fields cannot vary significantly on a substantially subwavelength scale, resulting in a nearly uniform transverse field profile (the width of the high refractive index region is $\sim\lambda/150$ for 1% fill factor). As the fill factor increases, the localization effect strengthens, reaching its maximum value of approximately 2.5 times that of the incident pulse at a fill factor of 6%. As the fill factor continues to increase, however, the increasing volume fraction of the high refractive index material results in a diminishing peak $|E|^2$. The peak $|E|^2$ values for fill factors varying from 1% to 12% are shown in Fig. 4. For fill factors larger than 12%, multiple transverse modes exist, significantly reducing the peak $|E|^2$. For the 9% fill factor case (corresponding to the results of Fig. 2), the peak value of $|E|^2$ is approximately 2.4 times that of the incident pulse, and over 12 times that of the bulk material case.

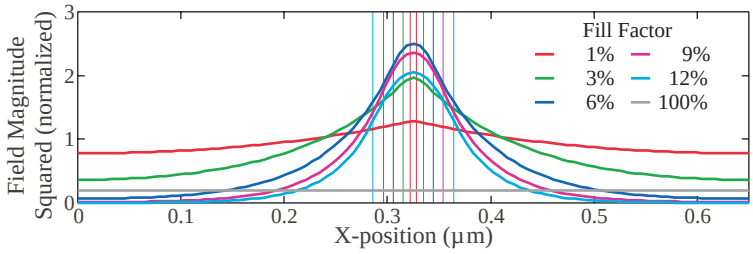

Fig. 3. Transverse profiles of the squared field magnitude at the pulse peak in one period of an infinitely periodic nanostructure for several fill factors. The grating period is 0.65 μm, and the normally incident pulse has a FWHM of 167 fs. The colored vertical lines indicate the respective boundaries of the high index region of the structure for the five fractional fill factors.

#22950 - $15.00 US
Received June 02, 2000; Revised July 26, 2000
(C) 2000 OSA

Fig. 4 shows the pulse group velocity inside the nanostructure as a function of the fill factor. As the fill factor increases from 1% to 12%, the group velocity decreases from almost $1.0c$ to roughly $0.3c$, where c is the speed of light. Thus, as the fraction of the pulse energy contained within the high refractive index material increases, the group velocity of the pulse in the nanostructure decreases. This behavior is similar to the dependence of the mode propagation speed on the guide thickness in a single-mode slab waveguide.

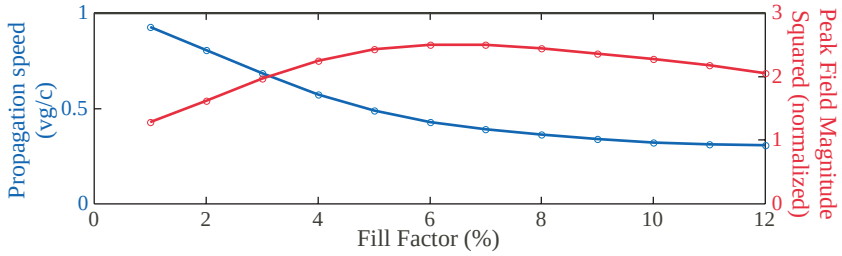

Fig. 4. Group velocity and peak field magnitude squared as a function of fill factor for a 167 fs FWHM pulse propagating in the structure of Fig. 1.

In applying the transverse field localization effect to the enhancement of nonlinear optical phenomena, we must also consider the volume fraction of nonlinear material. The intensity output of the second-harmonic generation (SHG) process is proportional to $|E|^4$. By integrating $|E|^4$ across the fraction of the grating period corresponding to the high refractive index material and comparing with the bulk case, we can obtain an effective SHG enhancement factor. The effective SHG enhancement factor for fill factors varying from 1% to 12% is shown in Fig. 5. A fill factor $F = 0.09$, corresponding to the results of Figs. 1 and 2, yields the maximum value of the SHG enhancement factor: approximately 10.8.

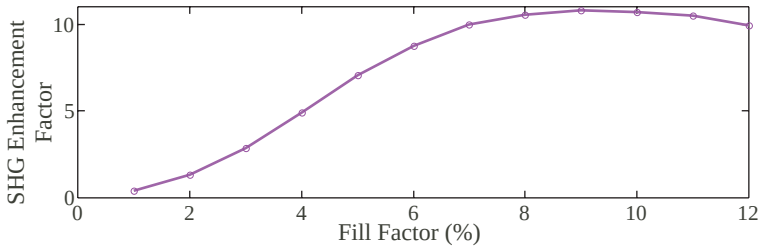

Fig. 5. SHG enhancement factor for the nanostructure of Fig. 1, with fill factor varying from 1% to 12%. The enhancement factor is computed by integrating $|E|^4$ over the part of the grating period corresponding to the high refractive index material, and normalizing to the bulk case.

5. Conclusions

We have presented an example optical nanostructure which imposes transverse near-field localization on incident ultrashort optical pulses. The elevation of the peak intensity of the pulse due to the transverse localization effect is used to complement the high peak power of an ultrashort optical pulse, with an application for enhancement of nonlinear optical phenomena. In addition, we briefly described the modeling method used to produce these results, consisting of an extension of the well-established RCWA method for the analysis of ultrashort optical pulses using Fourier spectrum decomposition. As this example suggests, interesting new phenomena and practical photonic devices may emerge from the combination of ultrashort optical pulses and near-field diffractive nanostructures.

#22950 - $15.00 US
Received June 02, 2000; Revised July 26, 2000
(C) 2000 OSA